












Genome Resources

A genome assembly of the Yuma myotis bat, *Myotis yumanensis*

Joseph N. Curti^{1,*}, Devaughn Fraser², Merly Escalona³, Colin W. Fairbairn⁴, Samuel Sacco⁴, Ruta Sahasrabudhe⁵, Oanh Nguyen⁵, William Seligmann⁴, Peter H. Sudmant⁶, Erin Toffelmier¹, Juan Manuel Vazquez⁶, Robert Wayne^{1,†}, H. Bradley Shaffer^{1,7} and Michael R. Buchalski⁸

¹Department of Ecology and Evolutionary Biology, University of California, Los Angeles (UCLA), Los Angeles, CA, United States,

²Connecticut Department of Energy and Environmental Protection, Hartford, CT, United States,

³Department of Biomolecular Engineering, University of California, Santa Cruz, Santa Cruz, CA, United States,

⁴Department of Ecology and Evolutionary Biology, University of California, Santa Cruz, Santa Cruz, CA, United States,

⁵DNA Technologies and Expression Analysis Core Laboratory, Genome Center, University of California, Davis, Davis, CA, United States,

⁶Department of Integrative Biology, University of California, Berkeley, Berkeley, CA, United States,

⁷Institute of the Environment and Sustainability, La Kretz Center for California Conservation Science, Institute of the Environment and Sustainability, University of California, Los Angeles (UCLA), Los Angeles, CA, United States,

⁸Wildlife Genetics Research Unit, Wildlife Health Laboratory, California Department of Fish and Wildlife, Sacramento, CA, United States

*Corresponding author: Department of Ecology and Evolutionary Biology, University of California, Los Angeles (UCLA), Los Angeles, CA, United States. Email: jcurti3@g.ucla.edu

†Deceased

Corresponding Editor: William Murphy

Abstract

The Yuma myotis bat (*Myotis yumanensis*) is a small vespertilionid bat and one of 52 species of new world *Myotis* bats in the subgenus *Pizonyx*. While *M. yumanensis* populations currently appear relatively stable, it is one of 12 bat species known or suspected to be susceptible to white-nose syndrome, the fungal disease causing declines in bat populations across North America. Only two of these 12 species have genome resources available, which limits the ability of resource managers to use genomic techniques to track the responses of bat populations to white-nose syndrome generally. Here we present the first de novo genome assembly for Yuma myotis, generated as a part of the California Conservation Genomics Project. The *M. yumanensis* genome was generated using a combination of PacBio HiFi long reads and Omni-C chromatin-proximity sequencing technology. This high-quality genome is one of the most complete bat assemblies available, with a contig N50 of 28.03 Mb, scaffold N50 of 99.14 Mb, and BUSCO completeness score of 93.7%. The Yuma myotis genome provides a high-quality resource that will aid in comparative genomic and evolutionary studies, as well as inform conservation management related to white-nose syndrome.

Key words: California Conservation Genomics Project, CCGP, chiroptera, long-read assembly, *Myotis yumanensis*, reference genome

Introduction

Bats (order Chiroptera) are the second-most diverse mammalian order, representing 22% of global mammal diversity (Simmons and Cirranello 2018; Mammal Diversity Database 2022). Despite their global distribution and ecological and economic importance, the conservation status of bats is less well understood than other species of mammals or birds (Frick et al. 2020). In step with data gaps in the global conservation status of bats, genomic resources for bats are also underdeveloped. Since the first reference genome of the little brown bat (*Myotis lucifugus*) was published by the Broad Institute in 2011 (Lindblad-Toh et al. 2011), 50 additional bat reference genomes have been made publicly available, although 37 (74%) of these genomes are highly fragmented,

primarily short-read assemblies. Eleven of the 19 currently recognized chiropteran families have at least one reference genome, and most are from species in the families Pteropodidae, Phyllostomidae, and Vespertilionidae, including four in the genus *Myotis*. Given that the genus contains more than 120 globally distributed species, many of which have experienced declines in recent decades, additional genomic resources are sorely needed for the group.

The Yuma myotis bat (hereafter “Yuma bat”; *Myotis yumanensis*; Allen 1864) is one of 47 bat species endemic to North America. The Yuma bat is abundant and widely distributed, occurring as far north as British Columbia, Canada, south throughout most of the western United States, and as far south as Morelos, Mexico (Braun et al. 2015). Yuma

Received July 12, 2023; Accepted September 13, 2023

© The American Genetic Association. 2023.

This is an Open Access article distributed under the terms of the Creative Commons Attribution-NonCommercial License (<https://creativecommons.org/licenses/by-nc/4.0/>), which permits non-commercial re-use, distribution, and reproduction in any medium, provided the original work is properly cited. For commercial re-use, please contact journals.permissions@oup.com

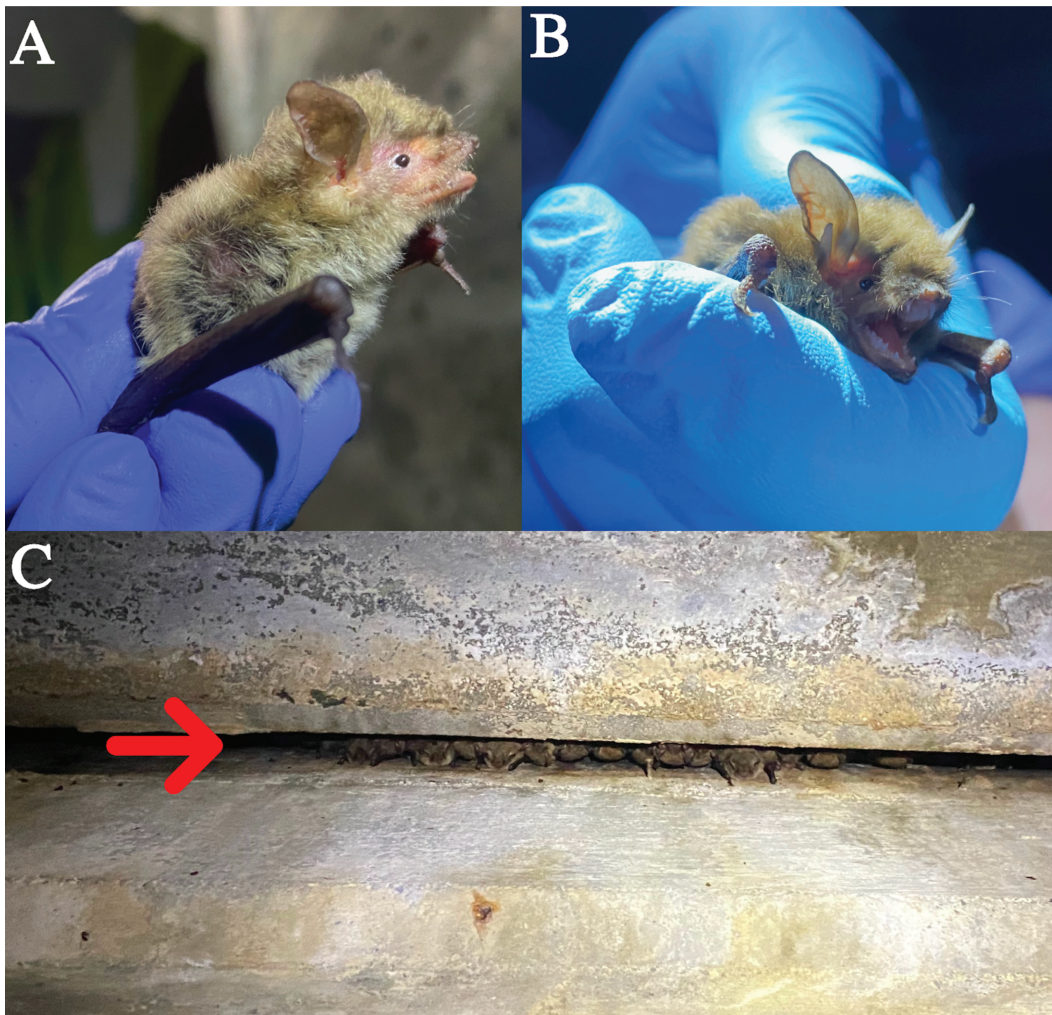


Fig. 1. (A) Profile view and (B) front-on view of Yuma myotis bats (*Myotis yumanensis*). (C) *M. yumanensis* day roost in a longitudinal joint of a bridge in Riverside County, California, USA.

bats are closely associated with riparian habitat for foraging (Brigham et al. 1992; Duff and Morrell 2007) and utilize a variety of natural (Braun et al. 2015) and manmade (Evelyn et al. 2004) roost types (Fig. 1). There are six putative subspecies of Yuma bat including *M. y. lambi*, *M. y. lutosus*, *M. y. oxalis*, *M. y. saturatus*, *M. y. sociabilis*, and *M. y. yumanensis*, although the extent to which these subspecies are supported as evolutionarily distinct lineages by genomic data is unknown (Braun et al. 2015).

The Yuma bat is also one of 12 bat species in North America with confirmed detection of *Pseudogymnoascus destructans* (Pd), the fungus responsible for white-nose syndrome (WNS). For some species of bats such as the little brown bat, WNS has resulted in more than 90% loss from certain colonies (Frick et al. 2010). Furthermore, although the IUCN considers the Yuma bat stable across its native range (Solarì 2019), occupancy models derived from acoustic data indicate a slight decline in summer occupancy over the three-year period of 2016–2019 (Udell et al. 2022). As WNS continues to spread across North America (Duncan 2023), it will be important to monitor common, abundant species such as the Yuma bat to detect and document population declines as they occur.

Genomic data provide an effective, efficient tool to monitor WNS-related mortalities in bat populations, as well as the genes

underlying survival. Using whole genome resequencing data, researchers have identified single nucleotide polymorphisms related to torpor and immune function in bat populations that survive WNS (Lilley et al. 2020b; Gignoux-Wolfsohn et al. 2021) and have investigated potential declines in genomic diversity following mass die offs (Lilley et al. 2020b). Genomic studies such as these rely heavily on the availability of high-quality reference genomes (Brandies et al. 2019).

Here, we describe the genome assembly for *M. yumanensis*, generated through the California Conservation Genomics Project (CCGP; Shaffer et al. 2022). One of the primary goals of the CCGP is to generate reference genomes and whole genome resequencing data for a comprehensive set of 153 ecologically and phylogenetically diverse species across California (Shaffer et al. 2022), and the Yuma bat is one of two chiropteran species in the project. Using PacBio HiFi long reads and Omni-C chromatin-proximity sequencing technology, we generated the first assembly for the species. The Yuma bat genome is an invaluable resource for basic research on diversification among *Myotis* species and the evolution of unique traits like echolocation and disease resistance, as well as more applied work on population size, connectivity, and genomic health that will aid in WNS management planning.

Methods

Tissue collection and cell culture

We captured a juvenile male Yuma bat from a maternity colony located in Chester, Plumas County, California. The specimen was collected by California Department of Fish and Wildlife (CDFW) staff under the department's jurisdiction as the trustee for wildlife management in the state of California, CA Fish & Game Code § 1802 (2015). The animal was transported to a CDFW laboratory facility where it was humanely euthanized via a combination of isoflurane and cervical dislocation. The carcass was immediately dissected and tissues were collected for genome sequencing. Several aliquots of kidney, lung, heart, spleen, liver, testes, intestine, skeletal muscle, and brain were washed sequentially in molecular grade water, ethanol, and water again before being flash frozen in liquid nitrogen. One aliquot of each tissue was reserved for generating primary cell cultures. Species identity was confirmed through Sanger sequencing of a fragment of the cytochrome oxidase subunit 1 (COI) mitochondrial gene using the methodology of Walker et al. (2016).

Primary cell cultures from the skin (plagiopatagium and body), heart, brain, cartilage, and eye were grown following Yohe et al. (2019) with modifications. Tissue samples were rinsed serially in baths of DPBS, 70% ethanol, and DPBS, and then stabilized in a cell culture medium consisting of BenchStable DMEM/F12 (Gibco Cat. #A4192002, ThermoFisher Scientific Inc., Waltham, MA) supplemented with 20% FBS (Gibco Cat. #26140087), 0.2% Primocin (InvivoGen Cat. #ant-pm-1, San Diego, CA), and 15 mM HEPES (Gibco Cat. #15630080). Tissues were minced in 500 μ L of DPBS using surgical scissors, and the tissues were digested overnight in 1 mg/mL Collagenase IV (Stemcell Technologies Cat. #07909, Vancouver, Canada) supplemented with 0.2% Primocin. The dissociated tissues were centrifuged at 500 \times g for 5 min, and washed twice with DPBS (Gibco Cat. #14190144). Cells were plated in T75 flasks containing cell culture media formulated as described, and grown in a 37 °C incubator with 5% CO₂ atmosphere.

Adherent cells were passaged four days post-collection ("Passage 0") using 0.05% Trypsin-EDTA (Gibco Cat. #25300054). Cells were then counted and replated in high glucose DMEM (Gibco Cat. #10569010) with pyruvate and GlutaMax supplementation, plus 10% FBS and 1% penicillin-streptomycin (Gibco Cat. #10378016). Three T175 flasks were seeded with approximately two million cells each after the first passage to generate triplicates of 10 million cell aliquots for DNA and RNA extraction.

Nucleic acid library preparation

High molecular weight genomic DNA (HMW gDNA) was isolated from cultured cells following a protocol described previously (Jain et al. 2018). Briefly, 10 million cultured skin fibroblast cells were lysed with 2 mL lysis buffer containing 10 mM NaCl, 25 mM EDTA, 0.5% (weight/volume) SDS, and 100 μ g/mL Proteinase K overnight at room temperature. The lysate was treated with RNase A for 30 min at 37 °C and cleaned with equal volumes of phenol/chloroform using phase lock gels (Quantabio Cat. #2302830, Beverly, MA). The HMW gDNA was precipitated by adding 0.4 \times volume of 5 M ammonium acetate and 3 \times volume of ice cold ethanol. The pellet was washed with 70% ethanol twice and resuspended in elution buffer (10 mM Tris, pH 8.0). The purity was assessed using NanoDrop spectrophotometer (260/280 = 1.8 and 260/230 = 2.0) and the integrity of the HMW gDNA was

verified on a Femto pulse system (Agilent Technologies, Santa Clara, CA).

The HiFi SMRTbell library was constructed using the SMRTbell Express Template Prep Kit v2.0 (Pacific Biosciences of California [PacBio] Cat. #100938900, Menlo Park, CA) according to the manufacturer's instructions. HMW gDNA was sheared to a target size distribution between 15 and 20 kb. The sheared gDNA was concentrated using 0.45 \times of AMPure PB beads (PacBio Cat. #100265900) for the removal of single-strand overhangs at 37 °C for 15 min, followed by further enzymatic steps of DNA damage repair at 37 °C for 30 min, end repair and A-tailing at 20 °C for 10 min and 65 °C for 30 min, ligation of overhang adapter v3 at 20 °C for 60 min and 65 °C for 10 min to inactivate the ligase, then nuclease treated at 37 °C for 1 h. The SMRTbell library was purified and concentrated with 0.45 \times AMPure PB beads for size selection using the BluePippin/PippinHT system (Sage Science Inc. Cat. #BLF7510/HPE7510, Beverly, MA) to collect fragments greater than 79 kb. The 15–20 kb average HiFi SMRTbell library was sequenced at the University of California, Davis, DNA Technologies Core (Davis, CA) using three SMRT Cell 8M Trays (PacBio Cat. #101389001), Sequel II sequencing chemistry 2.0, and 30-h movies each on a PacBio Sequel II sequencer.

The Omni-C library was prepared using a Dovetail Omni-C Kit (Dovetail Genomics Cat. #21005, Scotts Valley, CA) according to the manufacturer's protocol with slight modifications. First, cultured cell pellets (Sample ID: MYYU_CA2020_CCGP) were resuspended in 1 \times PBS. Then, chromatin was fixed in place in the nucleus, and the fixed chromatin was digested with DNase I and extracted. Chromatin ends were repaired and ligated to a biotinylated bridge adapter followed by proximity ligation of adapter-containing ends. After proximity ligation, crosslinks were reversed and the DNA was purified from proteins, purified DNA was treated to remove biotin that was not internal to ligated fragments, and a sequencing library was generated using the NEBNext Ultra II (New England Biolabs Inc. Cat. #E7645, Ipswich, MA) with an Illumina compatible γ -adaptor. Biotin-containing fragments were then captured using streptavidin beads. The post capture product was split into two replicates prior to PCR enrichment to preserve library complexity with each replicate receiving unique dual indices. The library was sequenced at the Vincent J. Coates Genomics Sequencing Laboratory (Berkeley, CA) on an Illumina NovaSeq 6000 platform (Illumina, San Diego, CA) to generate approximately 100 million 2 \times 150 bp read pairs per Gb of genome size.

Nuclear genome assembly

We assembled the *M. yumanensis* genome following the CCGP assembly pipeline Version 5.0, as outlined in Table 1, which lists the tools and nondefault parameters used. The pipeline uses PacBio HiFi reads and Omni-C data to produce high quality and highly contiguous genome assemblies. First, we removed the remnant adapter sequences from the PacBio HiFi dataset using HiFiAdapterFilt (Sim et al. 2022) and generated the initial dual or partially phased diploid assembly (<http://lh3.github.io/2021/10/10/introducing-dual-assembly>) using HiFiasm (Cheng et al. 2022) on Hi-C mode, with the filtered PacBio HiFi reads and the Omni-C dataset. We then aligned the Omni-C data to both assemblies following the Arima Genomics Mapping Pipeline

Table 1 Assembly pipeline and software used. Software citations are listed in the main text

Assembly	Software and any non-default options	Version
Filtering PacBio HiFi adapters	HiFiAdapterFilt	Commit 64d1c7b
K-mer counting	Meryl (k=21)	1
Estimation of genome size and heterozygosity	GenomeScope	2
De novo assembly (contiging)	HiFiasm (Hi-C Mode, --primary, output p_ctg.hap1, p_ctg.hap2)	0.16.1-r375
Scaffolding		
Omni-C data alignment	Arima Genomics Mapping Pipeline	Commit 2e74ea4
Omni-C scaffolding	SALSA (-DNASE, -i 20, -p yes)	2
Gap closing	YAGCloser (-mins 2 -f 20 -mcc 2 -prt 0.25 -eft 0.2 -pld 0.2)	Commit 0e34c3b
Omni-C contact map generation		
Short-read alignment	BWA-MEM (-5SP)	0.7.17-r1188
SAM/BAM processing	samtools	1.11
SAM/BAM filtering	pairtools	0.3.0
Pairs indexing	pairix	0.3.7
Matrix generation	cooler	0.8.10
Matrix balancing	hicExplorer (hicCorrectmatrix correct --filterThreshold -2 4)	3.6
Contact map visualization	HiGlass	2.1.11
	PretextMap	0.1.4
	PretextView	0.1.5
	PretextSnapshot	0.0.3
Genome quality assessment		
Basic assembly metrics	QUAST (--est-ref-size)	5.0.2
Assembly completeness	BUSCO (-m geno, -l mammalia)	5.0.0
	Merqury	2020-01-29
Contamination screening		
Local alignment tool	BLAST+ (-db nt, -outfmt '6 qseqid staxids bitscore std', -max_target_seqs 1, -max_hsp 1, -evalue 1e-25)	2.1
General contamination screening	BlobToolKit	2.3.3
Mitochondrial assembly		
Mitochondrial genome assembly	MitoHiFi (-r, -p 50, -o 1)	2.2
Comparing available genome assemblies		
Genome contiguity	ggplot2	3.4.1 (R version 4.2.3)
	Custom script (https://github.com/joeycurti3/myyu_joh)	Commit 3f5c8dd
Genome genic completeness	gVolante (-cutoff length = 1, -sequence type = Genome (nucleotide), -ortholog search pipeline = BUSCO v5, -ortholog set = mammalia)	2.0.0

(https://github.com/ArimaGenomics/mapping_pipeline) and scaffolded both assemblies with SALSA (Ghurye et al. 2017, 2019).

Both genome assemblies were manually curated by iteratively generating and analyzing their corresponding Omni-C contact maps. To generate the contact maps we aligned the Omni-C data with BWA-MEM (Li 2013), identified ligation junctions, and generated Omni-C pairs using pairtools (Open2C et al. 2023). We generated a multi-resolution Omni-C matrix with cooler (Abdennur and Mirny 2020) and balanced it with hicExplorer (Ramírez et al. 2018). We used HiGlass (Kerpedjiev et al. 2018) and the PretextSuite (<https://github.com/wtsi-hpag/PretextView>; <https://github.com/wtsi-hpag/PretextMap>; <https://github.com/wtsi-hpag/PretextSnapshot>) to visualize the contact maps where we identified misassemblies and misjoins, and finally modified the assemblies using the Rapid Curation pipeline from the Wellcome Trust Sanger Institute, Genome Reference Informatics Team (<https://gitlab.com/wtsi-grit/>

[rapid-curation](#)). Some of the remaining gaps (joins generated during scaffolding and curation) were closed using the PacBio HiFi reads and YAGCloser (<https://github.com/merlyescalona/yagcloser>). Finally, we checked for contamination using the BlobToolKit Framework (Challis et al. 2020).

Genome assembly assessment

We generated k-mer counts from the PacBio HiFi reads using meryl (<https://github.com/marbl/meryl>). The k-mer counts were then used in GenomeScope 2.0 (Ranallo-Benavidez et al. 2020) to estimate genome features including genome size, heterozygosity, and repeat content. To obtain general contiguity metrics, we ran QUAST (Gurevich et al. 2013). We evaluated genome quality and functional completeness using BUSCO (Manni et al. 2021) with the Mammalia ortholog database (mammalia_odb10) which contains 9,226 genes. Assessment of base level accuracy (QV) and k-mer completeness was

performed using the previously generated meryl database and mercurry (Rhie et al. 2020). We further estimated genome assembly accuracy via BUSCO gene set frameshift analysis using the pipeline described in Korlach et al. (2017). Measurements of the size of the phased blocks are based on the size of the contigs generated by HiFiasm on HiC mode. We followed the quality metric nomenclature established by Rhie et al. (2021), with the genome quality code $x \cdot y \cdot P \cdot Q \cdot C$, where, $x = \log_{10}[\text{contig NG50}]$; $y = \log_{10}[\text{scaffold NG50}]$; $P = \log_{10}[\text{phased block NG50}]$; $Q = \text{Phred base accuracy QV (quality value)}$; $C = \% \text{ genome represented by the first "n" scaffolds, following a karyotype of } 2n = 44$ (Braun et al 2015). Quality metrics for the notation were calculated on the assembly for Haplotype 1.

Mitochondrial genome assembly

We assembled the mitochondrial genome of *M. yumanensis* from the PacBio HiFi reads using the reference-guided pipeline MitoHiFi (Allio et al. 2020; Uliano-Silva et al. 2021). The mitochondrial sequence of an existing *M. yumanensis* (NCBI:NC_036319.1; Platt et al. 2018) was used as the starting reference sequence. After completion of the nuclear genome, we searched for matches of the resulting mitochondrial assembly sequence in the nuclear genome assembly using BLAST+ (Camacho et al. 2009) and filtered out contigs and scaffolds from the nuclear genome with a percentage of sequence identity >99% and size smaller than the mitochondrial assembly sequence.

Comparing available genome assemblies

We queried the National Library of Medicine's National Center for Biotechnology Information (NCBI) on 11 April 2023 for all representative genome assemblies using the taxon id for *Chiroptera* (search term: txid9397[Organism:exp]). For each assembly, we recorded the genomes's global statistics including genome size, scaffold number, scaffold N50, contig number, and contig N50. To compare the contiguity of available genomes, we accessed NCBI full sequence reports for all 50 available bat genomes and plotted the cumulative coverage of the genome by scaffold of a given size (NGx plot) in R (R Core Team 2022), using the package "ggplot2" (Wickham 2016) following scripts from Lin et al. (2022). To compare completeness of available genomes, we downloaded fasta sequences for all 50 available bat genomes on NCBI and we used gVolante (Nishimura et al. 2017, 2019) to run BUSCO using the Mammalian ortholog database (mammalia_odb10).

Results

The Omni-C and PacBio HiFi sequencing libraries generated 120.4 million read pairs and 4.7 million reads, respectively. The latter yielded ~40-fold coverage (N50 read length 16,323 bp; minimum read length 43 bp; mean read length 16,158 bp; maximum read length of 52,146 bp) based on the Genomescope 2.0 genome size estimation of 1.9 Gb. Based on PacBio HiFi reads, we estimated 0.194% sequencing error rate and 0.809% nucleotide heterozygosity rate. The k-mer spectrum based on PacBio HiFi reads show a bimodal distribution with two major peaks at ~38 and ~75-fold coverage, where peaks correspond to homozygous and heterozygous states of a diploid species (Fig. 2A).

The final assembly (mMyoYum1) consists of two partially phased haplotypes that vary slightly in size compared with the estimated value from GenomeScope 2.0 (Fig. 2A), as has been observed in other taxa (see e.g. Pflug et al. 2020). Haplotype 1 consists of 476 scaffolds spanning 1.94 Gb with contig N50 of 28.03 Mb, scaffold N50 of 99.14 Mb, longest contig of 120.09 Mb, and largest scaffold of 240.34 Mb. The Haplotype 2 assembly consists of 250 scaffolds, spanning 2.05 Gb with contig N50 of 26.79 Mb, scaffold N50 of 94.21 Mb, longest contig of 59.72 Mb, and largest scaffold of 216.39 Mb. Assembly statistics are reported in Table 2, and graphical representation for the primary assembly in Fig. 2B.

During manual curation, we generated a total of 12 breaks and 153 joins, with 6 breaks per haplotype, 79 joins for Haplotype 1, and 74 joins were made for Haplotype 2. We were able to close 45 gaps, 19 on Haplotype 1 and 26 on Haplotype 2, and we filtered out 2 contigs (1 per haplotype), corresponding to mitochondrial contamination. No further contigs were removed. The Omni-C contact maps show that both assemblies are highly contiguous (Fig. 2C and 2D). We have deposited both assemblies on NCBI (see Table 2 and Data Availability for details).

Haplotype 1 has a BUSCO completeness score of 93.7% using the Mammalian ortholog database, a per-base quality (QV) of 63.62, a kmer completeness of 89.64, and a frameshift indel QV of 40.98. Haplotype 2 has a BUSCO completeness score of 91.2% using the same ortholog database, a per-base quality (QV) of 63.88, a kmer completeness of 93.97, and a frameshift indel QV of 40.27. The Omni-C contact maps show that both assemblies are highly contiguous with some chromosome-length scaffolds (Fig. 2C and 2D, respectively; see Table 2 and Data availability for details).

The final mitochondrial genome size was 17,366 bp. The base composition of the final assembly version is $A = 33.55\%$, $C = 22.93\%$, $G = 13.44\%$, $T = 30.08\%$, and consists of 22 unique transfer RNAs and 13 protein-coding genes.

Across all available bat genomes, genome contiguity based on scaffold N50 values ranged from 0.0107 to 171.1 Gb ($\bar{x} = 29.73$). Furthermore, completeness based on BUSCO percentage of complete genes detected ranged from 47.33 to 96.61 ($\bar{x} = 85.39$). Generally, short-read genome assemblies were less contiguous ($\bar{x} = 11.03$ Mb) and less complete ($\bar{x} = 81.91$) than assemblies that used a combination of long and short reads ($\bar{x} = 92.44$ Mb and $\bar{x} = 95.21\%$, respectively).

Discussion

Here we provide the first genome assembly for the Yuma bat. This genome is highly contiguous and when compared against standards set by the Vertebrate Genome Project (VGP; <https://vertebrategenomesproject.org/>), this genome exceeds the proposed standards for the VGP2020 category (Rhie et al. 2021), with the exception of the "chromosome status" quality category, since we did not name or match chromosomes. This genomic resource is comparable in its contiguity and completeness to other modern de novo genome assemblies that use a combination of short and long-read technologies, and is one of the most contiguous bat genomes currently available based on scaffold N50 (99.14 Mb for Yuma bat, range of other taxa: 0.0107–171.1 Gb). When compared with the other available genomes for bats in the genus *Myotis*, this genome is the most contiguous based on scaffold N50 (99.14 Mb for Yuma bat, range of other taxa: 3.226–94.45 Mb; Fig.

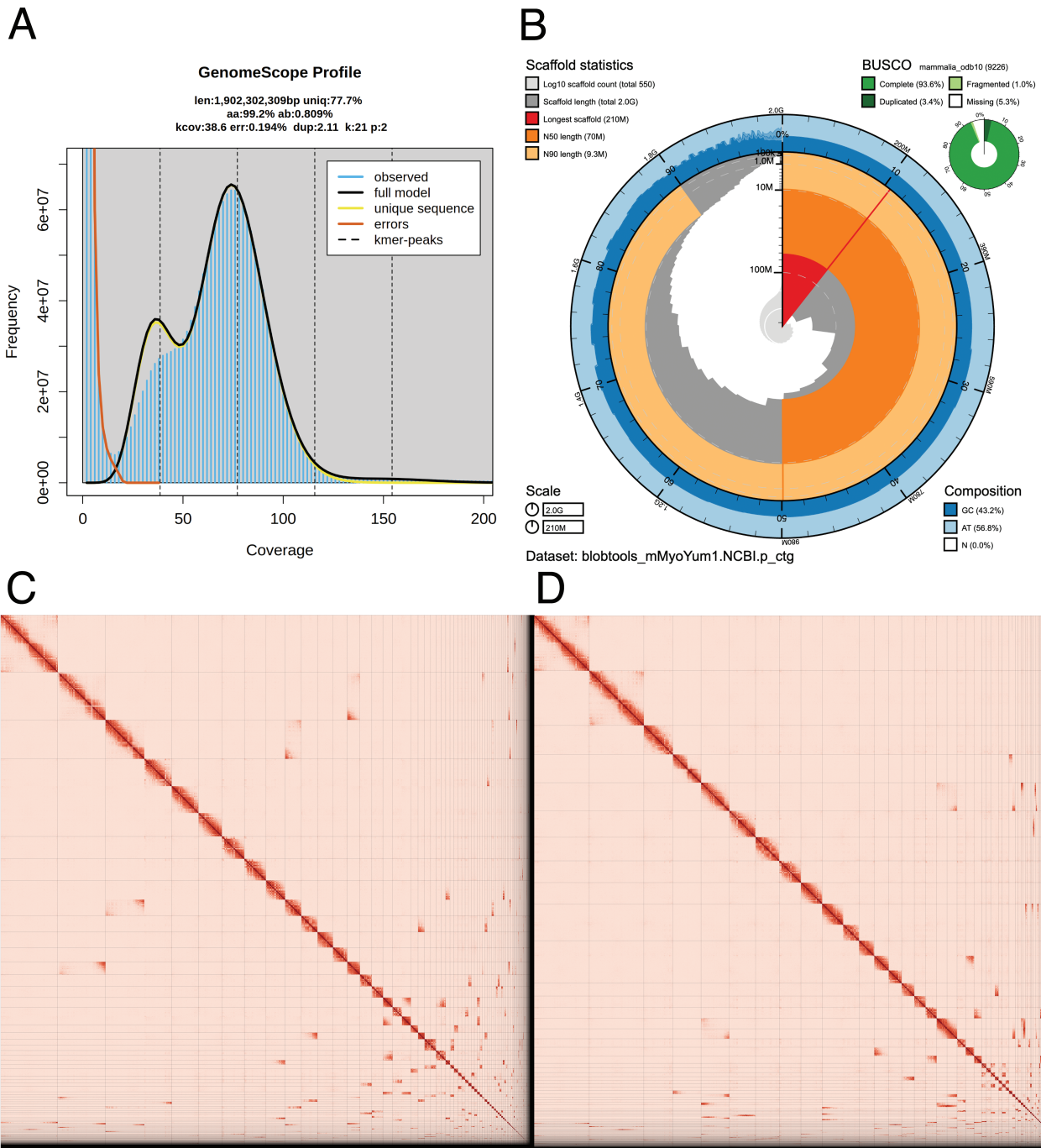


Fig. 2. Visual overview of genome assembly metrics. (A) K-mer spectra output generated from PacBio HiFi data without adapters using GenomeScope2.0. The bimodal pattern observed corresponds to a diploid genome. K-mers covered at lower coverage and lower frequency correspond to differences between haplotypes, whereas the higher coverage and higher frequency k-mers correspond to the similarities between haplotypes. (B) BlobToolKit Snail plot showing a graphical representation of the quality metrics presented in Table 2 for the *M. yumanensis* primary assembly (mMyoYum1.0.hap1). The plot circle represents the full size of the assembly. From the inside-out, the central plot covers length-related metrics. The red line represents the size of the longest scaffold; all other scaffolds are arranged in size-order moving clockwise around the plot and drawn in gray starting from the outside of the central plot. Dark and light orange arcs show the scaffold N50 and scaffold N90 values. The central light gray spiral shows the cumulative scaffold count with a white line at each order of magnitude. White regions in this area reflect the proportion of Ns in the assembly. The dark versus light blue area around it shows mean, maximum, and minimum GC versus AT content at 0.1% intervals (Challis et al. 2020). (C-D) The Omni-C contact map for the primary (C) and alternate (D) genome assemblies generated with PretextSnapshot. Omni-C contact maps translate proximity of genomic regions in 3D space to contiguous linear organization. Each cell in the contact map corresponds to sequencing data supporting the linkage (or join) between two such regions. Scaffolds are separated by black lines, and higher density corresponds to higher levels of fragmentation (See online version for color figure).

Table 2 Sequencing and assembly statistics, and accession numbers

Bio Projects & Vouchers	CCGP NCBI BioProject		PRJNA720569				
	Genera NCBI BioProject		PRJNA765635				
	Species NCBI BioProject		PRJNA777197				
	NCBI BioSample		SAMN30526064				
	Specimen identification		MYYU_CA2020_CCGP				
Genome Sequence	NCBI Genome accessions		Haplotype 1 (Primary)		Haplotype 2 (Alternate)		
	Assembly accession		JAPQVT000000000		JAPQVU000000000		
	Genome sequences		GCA_028538775.1		GCA_028536395.1		
Sequencing Data	PacBio HiFi reads	Run	1 PACBIO_SMRT (Sequel II) run: 4.7 M spots, 76.5 G bases, 57 Gb				
		Accession	SRX19740654				
	Omni-C Illumina reads	Run	2 ILLUMINA (Illumina NovaSeq 6000) runs: 120.5 M spots, 36.4 G bases, 11.9 Gb				
		Accession	SRX19740655, SRX19740656				
Genome Assembly Quality Metrics	Assembly identifier (Quality code [*])		mMyoYum1(7.7.P7.Q63.C96)				
	HiFi Read coverage ⁵		33.26X				
			Haplotype 1		Haplotype 2		
	Number of contigs		685		465		
	Contig N50 (bp)		28,025,655		26,795,370		
	Contig NG50 ⁵		28,147,841		28,130,932		
	Longest Contigs		120,097,812		597,242,388		
	Number of scaffolds		476		250		
	Scaffold N50		99,144,700		94,205,551		
	Scaffold NG50 ⁵		99,144,700		109,018,441		
	Largest scaffold		240,344,003		2,163,927,272		
	Size of final assembly		1,952,479,771		2,050,500,308		
	Phased block NG50 ⁵		27,204,636		27,189,810		
	Gaps per Gbp (# Gaps)		107 (209)		104 (215)		
	Indel QV (Frame shift)		40.98297536		40.27268042		
	Base pair QV		63.6294		63.8881		
			Full assembly = 63.76				
	k-mer completeness		89.6446		93.9753		
			Full assembly = 99.442				
	BUSCO completeness (mammalia) n = 9226			C	S	D	F
		H1 [‡]	93.70%	90.20%	3.50%	1.00%	5.30%
		H2 [‡]	95.80%	92.20%	3.60%	1.00%	3.20%
Organelles		1 complete mitochondrial sequence			CM053173.1		

^{*} Assembly quality code x.y.P.Q.C derived notation, from (Rhie et al. 2021). x = \log_{10} [contig NG50]; y = \log_{10} [scaffold NG50]; P = \log_{10} [phased block NG50]; Q = Phred base accuracy QV (Quality value); C = % genome represented by the first 'n' scaffolds, following a known karyotype for *M. yumanensis* of 2n = 44 (Braun et al 2015). Quality code for all the assembly denoted by Haplotype 1 assembly (mMyoYum1.0.hap1)

⁵ Read coverage and NGx statistics have been calculated based on the estimated genome size of 1.95 Gb

[‡] (H1) Haplotype 1 and (H2) Haplotype 2 assembly values.

3), and the second most complete based on its BUSCO score of 93.7% (range of other taxa: 86.57%–96.18%). Future work could further improve this assembly through additional manual curation of scaffold placement and targeted DNA-FISH to assign scaffolds to true karyotypes (Shakoori 2017). Such work, along with gene annotation using RNA-seq for gene prediction, is planned for future versions of this assembly.

Genomic data are increasingly being applied to investigate the unique traits bats possess, including the ability to act as hosts to many pathogens without succumbing

to illness (Chattopadhyay et al. 2020; Moreno Santillán et al. 2021), the physiological basis of unique feeding behaviors like sanguivory (blood feeding; Zepeda Mendoza et al. 2018), and the exceptional longevity of bats relative to their small body size (Foley et al. 2018; Sullivan et al. 2022). While these and other bat genomic studies have the potential to prove useful to human biomedical research as well as our understanding of chiropteran evolution, they are often severely limited by the availability and quality of genomic resources. For example, of the 50 bat reference genomes currently available, 34 (74%) are short-read

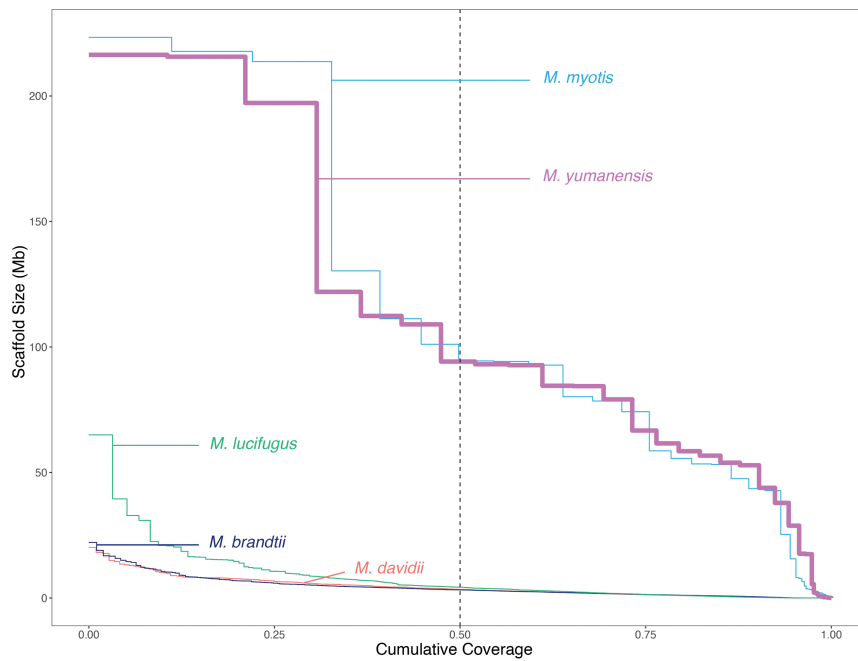


Fig. 3. NGx plot comparing contiguity of available de novo reference genomes for bats in the genus *Myotis*. The plot depicts the fraction of the genome (x-axis) that is covered by scaffolds of a given size in Mb (y-axis). The vertical dashed line depicts the N50 value, or half of the genome. The thick pink line is the genome of *M. yumanensis* presented in this paper.

assemblies with very low overall contiguity and completeness (Supplementary Materials). Our Yuma bat assembly provides a high quality, near-chromosome level resource in support of these research efforts. At the level of California biodiversity, the Yuma bat genome is the first chiropteran reference genome sequenced by the CCGP, filling a major gap in our emerging phylogeny of California biodiversity (Toffelmier et al. 2022). It contributes a new reference genome that will help in resolving outstanding questions on both species delimitation and phylogenetic relationships for the hyperdiverse genus *Myotis*, including the role of hybridization in shaping contemporary genomic architecture (Korstian et al. 2022). The CCGP will also generate 163 resequenced genomes throughout the species' distributional range, including all currently recognized subspecies, and this reference genome will be critical to evaluating the validity of, and relationships among, those taxa.

Genomic resources can also enhance the conservation and management of bat species, both in California (Fiedler et al. 2022) and globally. Two major foci of bat conservation are to better understand the susceptibility of individuals and species to WNS, and predict the spread of the pathogen among North American populations. Currently, only 5 of 20 bat species known to be affected by WNS have available genomic resources, including the reference genome presented here. Increasing genomic resources for these species will facilitate research on impacts of WNS, including the loss of genetic diversity due to population declines (Lilley et al. 2020b) and genomic predictions regarding individual-to-individual spread of the pathogen across landscapes (Lilley et al. 2020a).

In conclusion, we present the first high-quality genomic resource for the Yuma bat, a currently abundant and widespread North American species. This highly contiguous and complete de novo genome assembly will be a valuable

resource for studies aimed at understanding the evolution of unique bat traits and will contribute to bat conservation and management planning.

Supplementary material

Supplementary material can be found at <http://www.jhered.oxfordjournals.org/>.

Acknowledgements

PacBio Sequel II library prep and sequencing were carried out at the DNA Technologies and Expression Analysis Cores at the UC Davis Genome Center, supported by NIH Shared Instrumentation Grant 1S10OD010786-01. Deep sequencing of Omni-C libraries used the Novaseq S4 sequencing platforms at the Vincent J. Coates Genomics Sequencing Laboratory at UC Berkeley, supported by NIH S10 OD018174 Instrumentation Grant. We thank the staff at the UC Davis DNA Technologies and Expression Analysis Cores and the UC Santa Cruz Paleogenomics Laboratory for their diligence and dedication to generating high-quality sequence data. We also thank Dr. Courtney Miller for assistance with editing early drafts of this manuscript. This work used computational and storage services associated with the Hoffman2 Shared Cluster provided by UCLA Institute for Digital Research and Education's Research Technology Group.

Funding

This work was supported by the California Conservation Genomics Project, with funding provided to the University of California by the State of California, State Budget Act of 2019 [UC Award ID RSI-19-690224], and a White-nose Syndrome Recovery Research Grant [ID: F18AS00119]

awarded by the United States Fish and Wildlife Service to California Department of Fish and Wildlife. JMV was funded by a National Science Foundation Postdoctoral Research Fellowship in Biology [ID: 2109915].

Data availability

Data generated for this study are available under NCBI BioProject PRJNA777197. Raw sequencing data for sample MYYU_CA2020_CCGP (NCBI BioSample SAMN30526064) are deposited in the NCBI Short Read Archive (SRA) under SRX19740654 for PacBio HiFi sequencing data, and SRX19740655 and SRX19740656 for the Omni-C Illumina sequencing data. GenBank accessions for both primary and alternate assemblies are GCA_028538775.1 and GCA_028536395.1; and for genome sequences JAPQVT000000000 and JAPQVU000000000. Assembly scripts and other data for the analyses presented can be found at the following GitHub repository: www.github.com/ccgproject/ccgp_assembly.

References

- Abdennur N, Mirny LA. Cooler: scalable storage for Hi-C data and other genomically labeled arrays. *Bioinformatics*. 2020;36:311–316. <https://doi.org/10.1093/bioinformatics/btz540>.
- Allen H. Monograph of North American bats. *Smithsonian Misc Collect*. 1864;7:184.
- Allio R, Schomaker-Bastos A, Romiguier J, Prodocimi F, Nabholz B, Delsuc F. MitoFinder: efficient automated large-scale extraction of mitochondrial data in target enrichment phylogenomics. *Mol Ecol Resour*. 2020;20:892–905. <https://doi.org/10.1111/1755-0998.13160>.
- Brandies P, Peel E, Hogg CJ, Belov K. The value of reference genomes in the conservation of threatened species. *Genes*. 2019;10:846. <https://doi.org/10.3390/genes10110846>.
- Braun JK, Yang B, Gonzalez-Perez SB, Mares MA. *Myotis yumanensis* (Chiroptera: Vespertilionidae). *Mamm Species*. 2015;47:1–14. <https://doi.org/10.1093/mspecies/sev001>.
- Brigham RM, Aldridge HDJN, Mackey RL. Variation in habitat use and prey selection by yuma bats, *Myotis yumanensis*. *J Mammal*. 1992;73:640–645. <https://doi.org/10.2307/1382036>.
- Camacho C, Coulouris G, Avagyan V, Ma N, Papadopoulos J, Bealer K, Madden TL. BLAST+: architecture and applications. *BMC Bioinf*. 2009;10:421. <https://doi.org/10.1186/1471-2105-10-421>.
- Challis R, Richards E, Rajan J, Cochrane G, Blaxter M. BlobToolKit – interactive quality assessment of genome assemblies. *G3 Genes Genom Genet*. 2020;10:1361–1374.
- Chattopadhyay B, Garg KM, Ray R, Mendenhall IH, Rheindt FE. Novel de Novo genome of *Cynopterus brachyotis* reveals evolutionarily abrupt shifts in gene family composition across fruit bats. *Genome Biol Evol*. 2020;12:259–272. <https://doi.org/10.1093/gbe/evaa030>.
- Cheng H, Jarvis ED, Fedrigo O, Koepfli KP, Urban L, Gemmill NJ, Li H. Haplotype-resolved assembly of diploid genomes without parental data. *Nat Biotechnol*. 2022;40:1332–1335. <https://doi.org/10.1038/s41587-022-01261-x>.
- Duff AA, Morrell TE. Predictive occurrence models for bat species in California. *J Wildl Manag*. 2007;71:693–700. <https://doi.org/10.2193/2005-692>.
- Duncan, T. First Colorado bat tests positive for deadly white-nose syndrome. Colorado parks and wildlife; 2023. [accessed 2023 April 24]. <https://cpw.state.co.us/aboutus/Pages/News-Release-Details.aspx?NewsID=3797>.
- Evelyn MJ, Stiles DA, Young RA. Conservation of bats in suburban landscapes: roost selection by *Myotis yumanensis* in a residential area in California. *Biol Conserv*. 2004;115:463–473. [https://doi.org/10.1016/S0006-3207\(03\)00163-0](https://doi.org/10.1016/S0006-3207(03)00163-0).
- Fiedler PL, Erickson B, Esagro M, Gold M, Hull JM, Norris JM, Shapiro B, Westphal M, Toffelmier E, Shaffer HB. Seizing the moment: the opportunity and relevance of the California Conservation Genomics Project to state and federal conservation policy. *J Hered*. 2022;113:589–596.
- Foley NM, Hughes GM, Huang Z, Clarke M, Jebb D, Whelan CV, Petit EJ, Touzalin F, Farcy O, Jones G, et al. Growing old, yet staying young: the role of telomeres in bats' exceptional longevity. *Sci Adv*. 2018;4:eaao0926. <https://doi.org/10.1126/sciadv.aao0926>.
- Frick WF, Kingston T, Flanders J. A review of the major threats and challenges to global bat conservation. *Ann N Y Acad Sci*. 2020;1469:5–25. <https://doi.org/10.1111/nyas.14045>.
- Frick WF, Pollock JF, Hicks AC, Langwig KE, Reynolds DS, Turner GG, Butchkoski CM, Kunz TH. An emerging disease causes regional population collapse of a common North American bat species. *Science*. 2010;329:679–682. <https://doi.org/10.1126/science.1188594>.
- Ghurye J, Pop M, Koren S, Bickhart D, Chin C-S. Scaffolding of long read assemblies using long range contact information. *BMC Genomics*. 2017;18:527. <https://doi.org/10.1186/s12864-017-3879-z>.
- Ghurye J, Rhie A, Walenz BP, Schmitt A, Selvaraj S, Pop M, Phillippy AM, Koren S. Integrating Hi-C links with assembly graphs for chromosome-scale assembly. *PLoS Comput Biol*. 2019;15:e1007273. <https://doi.org/10.1371/journal.pcbi.1007273>.
- Gignoux-Wolfsohn SA, Pinsky ML, Kerwin K, Herzog C, Hall M, Bennett AB, Fefferman NH, Maslo B. Genomic signatures of selection in bats surviving white-nose syndrome. *Mol Ecol*. 2021;30:5643–5657. <https://doi.org/10.1111/mec.15813>.
- Gurevich A, Saveliev V, Vyahhi N, Tesler G. QUAST: quality assessment tool for genome assemblies. *Bioinformatics*. 2013;29:1072–1075. <https://doi.org/10.1093/bioinformatics/btt086>.
- Jain M, Koren S, Miga KH, Quick J, Rand AC, Sasani TA, Tyson JR, Beggs AD, Dilthey AT, Fiddes IT, et al. Nanopore sequencing and assembly of a human genome with ultra-long reads. *Nat Biotechnol*. 2018;36:338–345. <https://doi.org/10.1038/nbt.4060>.
- Kerpedjiev P, Abdennur N, Lekschas F, McCallum C, Dinkla K, Strobelt H, Luber JM, Ouellette SB, Azhir A, Kumar N, et al. HiGlass: web-based visual exploration and analysis of genome interaction maps. *Genome Biol*. 2018;19:125. <https://doi.org/10.1186/s13059-018-1486-1>.
- Korlach J, Gedman G, Kingan SB, Chin C-S, Howard JT, Audet J-N, Cantin L, Jarvis ED. De novo PacBio long-read and phased avian genome assemblies correct and add to reference genes generated with intermediate and short reads. *GigaScience*. 2017;6:1–16. <https://doi.org/10.1093/gigascience/gix085>.
- Korstian JM, Paulat NS, Platt RN, Stevens RD, Ray DA. SINE-based phylogenomics reveal extensive introgression and incomplete lineage sorting in myotis. *Genes*. 2022;13:399. <https://doi.org/10.3390/genes13030399>.
- Li H. Aligning sequence reads, clone sequences and assembly contigs with BWA-MEM, *arXiv*, arXiv:1303.3997 [q-Bio]. 2013. <https://doi.org/10.48550/arXiv.1303.3997>.
- Lilley TM, Sävilammi TM, Ossa G, Blomberg AS, Vasemägi A, Yung V, Vendrami D, Johnson JS. Population connectivity predicts vulnerability to white-nose syndrome in the Chilean *Myotis chiloensis*—a genomics approach. *G3 Genes Genom Genet*. 2020a;10:2117–2126. <https://doi.org/10.25387/G3.12173385>.
- Lilley TM, Wilson IW, Field KA, Reeder DM, Vodzak ME, Turner GG, Kurta A, Blomberg AS, Hoff S, Herzog CJ, et al. Genome-wide changes in genetic diversity in a population of *Myotis lucifugus* affected by white-nose syndrome. *G3 Genes Genom Genet*. 2020b;10:2007–2020. <https://doi.org/10.1534/g3.119.400966>.
- Lin M, Escalona M, Sahasrabudhe R, Nguyen O, Beraut E, Buchalski MR, Wayne RK. A reference genome assembly of the bobcat, *Lynx rufus*. *J Hered*. 2022;113:615–623. <https://doi.org/10.1093/jhered/esac031>.
- Lindblad-Toh K, Garber M, Zuk O, Lin MF, Parker BJ, Washietl S, Kheradpour P, Ernst J, Jordan G, Mauriceli E, et al. (2011). A high-resolution map of human evolutionary constraint using 29

- mammals. *Nature*, 478:476–482. <https://doi.org/10.1038/nature10530>.
- Mammal Diversity Database. (2022). *Mammal diversity database (Version 1.9)*. Zenodo. <http://doi.org/10.5281/zenodo.4139818>.
- Manni M, Berkeley MR, Seppy M, Simão FA, Zdobnov EM. BUSCO Update: novel and streamlined workflows along with broader and deeper phylogenetic coverage for scoring of eukaryotic, prokaryotic, and viral genomes. *Mol Biol Evol*. 2021;38:4647–4654. <https://doi.org/10.1093/molbev/msab199>.
- Moreno Santillán DD, Lama TM, Gutierrez Guerrero YT, Brown AM, Donat P, Zhao H, Rossiter SJ, Yohe LR, Potter JH, Teeling EC, et al. Large-scale genome sampling reveals unique immunity and metabolic adaptations in bats. *Mol Ecol*. 2021;30:6449–6467. <https://doi.org/10.1111/mec.16027>.
- Nishimura O, Hara Y, Kuraku S. GVolante for standardizing completeness assessment of genome and transcriptome assemblies. *Bioinformatics*. 2017;33:3635–3637. <https://doi.org/10.1093/bioinformatics/btx445>.
- Nishimura O, Hara Y, Kuraku S. Evaluating genome assemblies and gene models using gvolante. In: Kollmar M, editor. *Gene prediction: methods and protocols*. Vol. 1962. New York (NY): Springer; 2019. p. 247–256. <https://doi.org/10.1007/978-1-4939-9173-0>
- Open2C, Abdennur N, Fudenberg G, Flyamer IM, Galitsyna A A, Goloborodko A, Imakaev M, Venev SV. Pairtools: From sequencing data to chromosome contacts. *bioRxiv*. 2023. <https://doi.org/10.1101/2023.02.13.528389>.
- Pflug JM, Holmes VR, Burrus C, Johnston JS, Maddison DR. Measuring genome sizes using read-depth, k-mers, and flow cytometry: methodological comparisons in beetles (Coleoptera). *G3 Genes Genom Genet*. 2020;10:3047–3060. <https://doi.org/10.1534/g3.120.401028>.
- Platt RN, Faircloth BC, Sullivan KAM, Kieran TJ, Glenn TC, Vandeweghe MW, Lee TE, Baker RJ, Stevens RD, Ray DA. Conflicting evolutionary histories of the mitochondrial and nuclear genomes in new world *Myotis* bats. *Syst Biol*. 2018;67:236–249. <https://doi.org/10.1093/sysbio/syx070>.
- R Core Team. (2022) *R: A Language and Environment for Statistical Computing*. R Foundation for Statistical Computing. <https://www.R-project.org/>.
- Ramírez F, Bhardwaj V, Arrigoni L, Lam KC, Grüning BA, Villaveces J, Habermann B, Akhtar A, Manke T. High-resolution TADs reveal DNA sequences underlying genome organization in flies. *Nat Commun*. 2018;9:189. <https://doi.org/10.1038/s41467-017-02525-w>.
- Ranallo-Benavidez TR, Jaron KS, Schatz MC. GenomeScope 2.0 and Smudgeplot for reference-free profiling of polyploid genomes. *Nat Commun*. 2020;11:1432. <https://doi.org/10.1038/s41467-020-14998-3>.
- Rhie A, McCarthy SA, Fedrigo O, Damas J, Formenti G, Koren S, Uliano-Silva M, Chow W, Functammasan A, Kim J, et al. Towards complete and error-free genome assemblies of all vertebrate species. *Nature*. 2021;592:737–746. <https://doi.org/10.1038/s41586-021-03451-0>.
- Rhie A, Walenz BP, Koren S, Phillippy AM. Merqury: reference-free quality, completeness, and phasing assessment for genome assemblies. *Genome Biol*. 2020;21:245. <https://doi.org/10.1186/s13059-020-02134-9>.
- Shaffer HB, Toffelmier E, Corbett-Detig RB, Escalona M, Erickson B, Fiedler P, Gold M, Harrigan RJ, Hodges S, Luckau TK, et al. Landscape genomics to enable conservation actions: the California conservation genomics project. *J Hered*. 2022;113:577–588. <https://doi.org/10.1093/jhered/esac020>.
- Shakoori AR. Fluorescence in situ hybridization (FISH) and its applications. In: Bhat T, Wani A, editors. *Chromosome structure and aberrations*. New Delhi: Springer, 2017. https://doi.org/10.1007/978-81-322-3673-3_16.
- Sim SB, Corpuz RL, Simmonds TJ, Geib SM. HiFiAdapterFilt, a memory efficient read processing pipeline, prevents occurrence of adapter sequence in PacBio HiFi reads and their negative impacts on genome assembly. *BMC Genomics*. 2022;23:157. <https://doi.org/10.1186/s12864-022-08375-1>.
- Simmons NB, Cirranello AL. *Bat species of the world: a taxonomic and geographic database*; 2018 [accessed 2023 April 5]. <https://batnames.org/>
- Solari, S. *Myotis yumanensis*. The IUCN red list of threatened species 2019: e.T14213A22068335; 2019. <http://doi.org/10.2305/IUCN.UK.2019-1.RLTS.T14213A22068335.en>
- Sullivan IR, Adams DM, Greville LJS, Faure PA, Wilkinson GS. Big brown bats experience slower epigenetic aging during hibernation. *Proc R Soc B Biol Sci*. 2022;289:20220635. <https://doi.org/10.1098/rspb.2022.0635>.
- Toffelmier E, Beninde J, Shaffer HB. The phylogeny of California, and how it informs setting multi-species conservation priorities. *J Hered*. 2022;113:597–603. <https://doi.org/10.1093/jhered/esac045>.
- Udell BJ, Straw BR, Cheng TL, Enns K, Gotthold B, Irvine KM, Lausen C, Loeb S, Reichard J, Rodhouse T, et al. *Summer occupancy analysis 2010-2019 (status and trends of North American bats)*. Fort Collins, CO: North American Bat Monitoring Program; 2022. p. 248.
- Uliano-Silva M, Ferreira JGRN, Krashenninnikova K, Darwin Tree of Life Consortium, Blaxter M, Mieszkowska N, Hall N, Holland P, Durbin R, Richards T, et al. MitoHiFi: A python pipeline for mitochondrial genome assembly from PacBio high fidelity reads. *BMC Bioinformatics*. 2023;24:288. <https://doi.org/10.1186/s12859-023-05385-y>.
- Walker FM, Williamson CHD, Sanchez DE, Sobek CJ, Chambers CL. Species from feces: order-wide identification of chiroptera from guano and other non-invasive genetic samples. *PLoS One*. 2016;11:e0162342. <https://doi.org/10.1371/journal.pone.0162342>.
- Wickham, H. *ggplot2: elegant graphics for data analysis*. New York (NY): Springer-Verlag; 2016. <https://ggplot2.tidyverse.org>
- Yohe LR, Devanna P, Davies KTJ, Potter JHT, Rossiter SJ, Teeling EC, Vernes SC, Dávalos LM. Tissue collection of bats for -omics analyses and primary cell culture. *J Vis Exp*. 2019;152:59505. <https://doi.org/10.3791/59505>.
- Zepeda Mendoza ML, Xiong Z, Escalera-Zamudio M, Runge AK, Thézé J, Streicker D, Frank HK, Loza-Rubio E, Liu S, Ryder OA, et al. Hologenic adaptations underlying the evolution of sanguivory in the common vampire bat. *Nature Ecol Evol*. 2018;2:659–668. <https://doi.org/10.1038/s41559-018-0476-8>.